Field theory of enzyme-substrate systems with restricted long-range interactions

Fabrizio Olmeda[*]

Max Planck Institute for the Physics of Complex Systems, D-01138 Dresden, Germany
and Institute of Science and Technology Austria, 3400 Klosterneuberg, Austria

Steffen Rulands [†]

Arnold Sommerfeld Center for Theoretical Physics and Center for NanoScience, Department of Physics,
Ludwig-Maximilians-Universität München, D-80333 Munich, Germany
and Max Planck Institute for the Physics of Complex Systems, D-01138 Dresden, Germany

Enzyme-substrate kinetics form the basis of many biomolecular processes. The interplay between substrate binding and substrate geometry can give rise to long-range interactions between enzyme binding events. Here we study a general model of enzyme-substrate kinetics with restricted long-range interactions described by an exponent $-\gamma$. We employ a coherent-state path integral and renormalization group approach to calculate the first moment and two-point correlation function of the enzyme-binding profile. We show that starting from an empty substrate the average occupancy follows a power law with an exponent $1/(1-\gamma)$ over time. The correlation function decays algebraically with two distinct spatial regimes characterized by exponents $-\gamma$ on short distances and $-(2/3)(2-\gamma)$ on long distances. The crossover between both regimes scales inversely with the average substrate occupancy. Our work allows associating experimental measurements of bound enzyme locations with their binding kinetics and the spatial conformation of the substrate.

I. INTRODUCTION

The binding of enzymes to substrates can catalyze chemical reactions. Enzyme-substrate kinetics therefore form the basis of many biochemical processes. Such kinetics include, for example, the binding of polymerase molecules to the DNA for the transcription of genes to messenger ribonucleic acid molecules [1], the binding of oxidase enzymes to the outer membrane of mitochondria for the oxidation of monoamines, or the multisite phosphorylation of proteins [2].

Enzymes can interact in many ways when binding to the substrate. Transcription factors, which control the transcription of genes, often need to bind combinatorically together with other transcription factors in order to initiate transcription [3]. Some enzymes seem to slide diffusively along the substrate, such as the DNA methyl transferase DNMT1 [4]. In many biologically relevant scenarios, the substrate undergoes conformational changes when bound by an enzyme [5]. This is, for example, used to increase the specificity of enzyme binding in a kinetic proofreading scheme [6]. Many enzymes

that bind to the DNA, including chromatin modifiers, cause conformation changes thereof, most notably the compaction and decompaction of the DNA [7]. Positions that are far apart measured along the DNA sequence might then be close in physical space. Due to the feedback of enzyme binding with chromatin conformation, this gives rise to effective long-range interactions between binding events. Long-range interactions originating from fluctuating substrates are also known to drive the formation of ParB condensates in bacterial cells [8–10] and the formation of epigenetic domains via chromatin remodeling [11,12].

Experimentally, novel technologies in molecular biology allow quantifying the binding locations of enzymes to substrates like membranes or the DNA in a static manner. These technologies include super-resolution microscopy such as DNA Paint [13], which can image a wide range of enzyme binding events with the resolution of individual enzymes [14]. For one-dimensional substrates, single-cell sequencing technologies allow measuring the consequences of enzyme binding, such as chemical modifications of the DNA or histone tails, with the resolution of single base pairs and in individual cells [15,16]. A theoretical prediction about the relation between the statistics of bound positions on the substrate and the kinetics of enzyme binding would set the basis for concluding the enzyme kinetics and substrate conformation from such experiments.

In thermal equilibrium, the binding and unbinding of enzymes are strictly constrained by the condition of detailed balance. In this case, the equilibrium enzyme binding profile is predicted by the Gibbs free energy [17]. In the context of cell

---
[*]Contact author: fabrizio.olmeda@ista.ac.at
[†]Contact author: rulands@lmu.de

biology, enzyme-substrate kinetics is often out of equilibrium. Prominent examples of such kinetics are chromatin modifiers, which catalyze the irreversible deposition of epigenetic marks on the DNA or histone tails and may lead to conformational changes of the DNA. In these cases, a description in terms of thermodynamic potentials is not feasible and the theory of stochastic processes provides a general framework for describing nonequilibrium enzyme-substrate kinetics [18–21].

Biological substrates and enzymes are often highly nonlinear and the spatial dimensions cannot be neglected [21–26]. In these cases, standard approximation schemes of master equations and Langevin equations do not exist or are difficult to use. In these cases, path-integral representations of stochastic processes provide a versatile and powerful framework for studying stochastic processes. These include the Martin-Siggia-Rose-Janssen-de Dominicis functional integral representation of stochastic differential equations and the coherent-state path integral representation of master equations [27]. In both cases, expectation values of observables can be expressed in terms of deterministic path integrals over a pair of conjugated fields. Path-integral representations allow for the application of powerful theoretical tools, such as perturbation theory and renormalization group theory [28], in the context of stochastic processes.

In this work, we develop a theoretical framework of the out-of-equilibrium enzyme-binding kinetics on substrates. Specifically, we use a coherent-state path-integral approach in combination with renormalization-group calculations to obtain the moments of the distribution of enzymes bound on the substrate. We show that the first moment, the fraction of bound sites, increases according to a power law with an exponent depending on the decay exponent of long-range interactions. The two-point correlation function decays in two temporal regimes characterized by different exponents. For short distances, it is dominated by active feedback between enzyme binding events, and for long distances by conservative noise.

II. MODEL DEFINITION

We consider a general model for enzyme-substrate kinetics. In this model, the substrate is represented by a one-dimensional lattice of size N. On this lattice, each position is a potential binding site indexed by $i \in \{1, \dots, N\}$. Enzymes can bind to and unbind from lattice sites with rates that depend on the positions of other bound enzymes. This dependence of the binding rates is encoded in an interaction kernel J_{ij} which gives the contribution of a bound enzyme at position j to the enzyme binding rate at position i [Fig. 1(a)].

We here restrict interactions to the nearest bound sites, specifically, if the nearest bound sites are at positions j_1 and j_2, then the interaction kernel is $J_{i,j_1} + J_{i,j_2}$, where the two terms correspond to the contribution from the left and right bound neighbor, respectively. Such interactions are in the literature known as restricted long-range interactions [29–31]. A restriction of the interaction range is plausible both for physical and biological reasons. Physically, a restriction of the interaction range is required to adequately define the thermodynamic limit for interactions that decay with an exponent that is smaller than the dimension of the system [32]. Biologically, interactions are often restricted in range due to
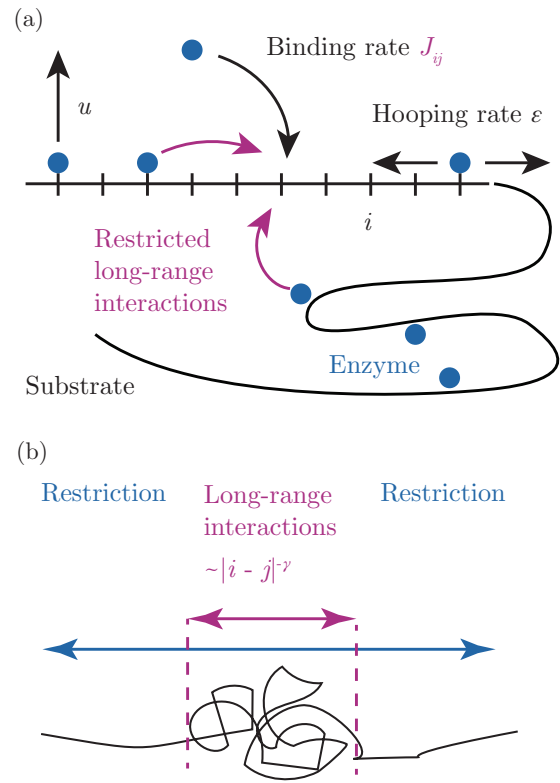

FIG. 1. (a) Schematic depicting the stochastic enzyme-substrate model. In this model, enzymes bind to a substrate with a binding rate that depends on the distance to the nearest bound sites. In the context of cell biology, substrates like DNA have dynamic geometries, such that local interactions in space lead to long-range interactions along the linear lattice. (b) If the size of compacted regions of the substrate is associated with a characteristic length scale, then long-range interactions are restricted to that length scale.

an effectively finitely sized substrate. For example, in the formation of epigenetic domains the presence of nucleosomes limits the interaction between enzymes [33] to regions much smaller than the total length of the DNA molecule. On the scale of tens of nanometers nucleosomes from structures that have been described as clutches and that are separated by regions of open chromatin [34]. Beyond a length scale that is defined by the characteristic size of these clutches the rate of interactions between genomic loci is reduced [Fig. 1(b)]. While the statistics of chromatin interactions on the scale of tens of nano meters is poorly understood the restricted long-range interactions we study in this manuscript describe such scenarios heuristically.

We further only consider translationally invariant kernels of the form $J(|i - j|)$. The unbinding rate of the enzyme is constant and we denote it by u. In equilibrium, the binding and unbinding rates would be related by the condition of detailed balance. Here, since many enzymatic processes are microscopically irreversible through the conversion of ATP to ADP, we do not make this assumption and take the unbinding rate to be independent. We further allow enzymes to perform random walks along the substrate with a rate ϵ.

With this, the state of the system is described by a random vector $\boldsymbol{\sigma}$ with entries representing enzyme occupancy: $\sigma_i = 1$

if site i is bound and $\sigma_i = 0$ otherwise. The time evolution of the probability of finding a given binding profile $\boldsymbol{\sigma}$ at a time t then follows a master equation of the form

$$
\frac{\partial P(\boldsymbol{\sigma})}{\partial t} = \sum_{i=1}^{N} \sum_{l=i+1}^{N} J_{i,i+l} \left(\prod_{j=1}^{l-1} \bar{\sigma}_{i+j} \right) \sigma_l [\sigma_i P(\bar{\boldsymbol{\sigma}}_i) - \bar{\sigma}_i P(\boldsymbol{\sigma})] + \sum_{i=1}^{N} \sum_{l=1}^{i-1} J_{i,i-l} \left(\prod_{j=1}^{l} \bar{\sigma}_{i-j} \right) \sigma_l [\sigma_i P(\bar{\boldsymbol{\sigma}}_i) - \bar{\sigma}_i P(\boldsymbol{\sigma})]
$$

$$
+ \epsilon \sum_{i=1}^{N} [\bar{\sigma}_i \sigma_{i+1} P(\bar{\boldsymbol{\sigma}}_i) - \sigma_i \bar{\sigma}_{i-1} P(\bar{\boldsymbol{\sigma}}_{i-1})] + \epsilon \sum_{i=1}^{N} [\bar{\sigma}_i \sigma_{i+1} P(\bar{\boldsymbol{\sigma}}_i) - \sigma_i \bar{\sigma}_{i+1} P(\bar{\boldsymbol{\sigma}}_{i+1})] + u \sum_{i=1}^{N} \sigma_i [P(\bar{\boldsymbol{\sigma}}_i) - P(\boldsymbol{\sigma})]. \quad (1)
$$

Here we introduced a notation for the vector $\bar{\boldsymbol{\sigma}}_i$ which has the same elements as $\boldsymbol{\sigma}$, but the value of σ_i at position i is replaced by $1 - \sigma_i$. Similarly, we define $\bar{\sigma}_i = 1 - \sigma_i$. In Eq. (1) the first and second terms describe interactions with the right and left nearest neighbor, respectively. The third and fourth terms describe the random walk of enzymes along the substrate and the final term describes enzyme unbinding events.

III. COHERENT-STATE PATH INTEGRAL FORMULATION OF THE MASTER EQUATION

Having defined a general model for the kinetics of enzyme-substrate binding in terms of Eq. (1), we now investigate the nonstationary distribution $P(\boldsymbol{\sigma}, t)$ in terms of its moments. To this end, we employ a coherent-state path integral formulation of the master equation, Eq. (1) [27]. Taking the semiclassical limit we will compare the prediction for the first- and higher-order moments to numerical simulations.

To define the path-integral representation we first introduce a Fock space, in which we represent lattice configurations in bra-ket notation. We define creation operators $a_i^{\dagger}$ which formally represent the binding of enzymes to site i. With these, we can express a given state $|\sigma\rangle = |\sigma_1, \ldots, \sigma_N\rangle$ as the repeated application of creation operators on the empty lattice, $|0\rangle$,

$$
|\sigma\rangle = a_1^{\dagger \sigma_1} \cdots a_N^{\dagger \sigma_N} |0\rangle. \quad (2)
$$

We also define annihilation operators, a_i, which represent the unbinding of enzymes from a given site i. The annihilation operators are conjugate to the creation operators, such that both act on a given lattice configuration as follows:

$$
\begin{aligned}
a_i^{\dagger} |\sigma\rangle &= |\sigma_i + 1\rangle, \\
a_i |\sigma\rangle &= \sigma_i |\sigma_i - 1\rangle. \quad (3)
\end{aligned}
$$

With these definitions, the creation and annihilation operators follow standard commutation rules,

$$
[a_i, a_i^{\dagger}] = 1. \quad (4)
$$

We can now write the probability distribution in Fock space formally as [35]

$$
|P(t)\rangle = \sum_{\boldsymbol{\sigma}} P(\boldsymbol{\sigma}, t) a_1^{\dagger \sigma_1} \ldots a_N^{\dagger \sigma_N} |0\rangle. \quad (5)
$$

Using this notation, we can formally rewrite the master equation in terms of the creation and annihilation operators,

$$
\partial_t |P(t)\rangle = -H |P(t)\rangle, \quad (6)
$$

with a "Hamiltonian" H defined as

$$
\begin{aligned}
H = &\sum_{i=1}^{N} \sum_{l=1}^{N-i} J_{i,i+l} \prod_{j=1}^{l-1} [(1 - a_{i+j}^{\dagger} a_{i+j}) \\
&\cdot a_{i+l}^{\dagger} a_{i+l} (a_i^{\dagger} \hat{\delta}_{\sigma_i,0} - \hat{\delta}_{\sigma_i,0})] \\
&+ \sum_{i=1}^{N-1} \epsilon (1 - a_i a_{i+1}^{\dagger}) \hat{\delta}_{\sigma_i,1} \delta_{\sigma_{i+1},0} \\
&+ \sum_{i=1}^{N-1} \epsilon (1 - a_i a_{i-1}^{\dagger}) \hat{\delta}_{\sigma_i,1} \delta_{\sigma_{i-1},0} \\
&+ \sum_{i=1}^{N} \sum_{l=1}^{i-1} J_{i,l} \prod_{j=1}^{l} [(1 - a_{i-j}^{\dagger} a_{i-j}) \cdot a_{i-l}^{\dagger} a_{i-l}]. \quad (7)
\end{aligned}
$$

The operators, $\hat{\delta}_{\sigma_i,k}$ are equal to the identity if a site i is occupied by k enzymes and 0 otherwise. These operators enforce that only a single enzyme can be bound at a given site. Although we will refer to H as a Hamiltonian, H does not represent an energy as it is not necessarily Hermitian unless detailed balance is fulfilled.

With this, we can write the expectation value of any observable $A(\boldsymbol{\sigma}, t)$ as

$$
\langle A(\boldsymbol{\sigma}, t)\rangle = \sum_{\boldsymbol{\sigma}} A(\boldsymbol{\sigma}) P(\boldsymbol{\sigma}, t). \quad (8)
$$

We can rewrite this equation as

$$
\langle A(\boldsymbol{\sigma}, t)\rangle = \langle 0| \prod_i \sigma_i e^{a_i} A(\boldsymbol{\sigma}) |P(t)\rangle, \quad (9)
$$

where we introduce a coherent state basis $\langle 0|e^a$, which has the property to be the left eigenstate of the creation operator $a^{\dagger}$,

$$
\langle 0|e^a a^{\dagger} = \sum_{n=1}^{\infty} \frac{\langle 0|}{n!} a^n a^{\dagger} = \langle 0|e^a. \quad (10)
$$

Having defined all the rules of the operators (cf. Appendix A) we now proceed to derive the path-integral representation of the master equation. To this end, we define a continuous field, $\phi_i(t)$, giving the local density of bound sites at position i. We then use the decomposition of 1,

$$
1 = \int d\phi_i \, d\hat{\phi}_i \, e^{-\hat{\phi}_i \phi_i} e^{\phi_i a_i^{\dagger}} |0\rangle \langle 0| e^{\hat{\phi}_i a_i}, \quad (11)
$$

to derive a path-integral representation of the master equation following standard steps [35,36]. This decomposition introduces a second field, $\hat{\phi}$, which is called the response field or conjugated field. In this path-integral representation

the moments of the distribution $P(\boldsymbol{\phi}, t)$ can be expressed in terms derivatives of the generating functional [37,38],

$$Z[\boldsymbol{h}, \phi, \hat{\phi}] = \int \mathcal{D}[\boldsymbol{h}, \phi, \hat{\phi}] e^{-S[\phi, \hat{\phi}] + \int dt \sum_i [h_i \phi_i + \hat{h}_i \hat{\phi}_i]}, \quad (12)$$

where we used the notation $\mathcal{D}[\boldsymbol{h}, \phi, \hat{\phi}]$ to denote the integrals over all positions $\prod_i d\phi_i d\hat{\phi}_i dh_i$. The argument in the exponential is an action of the form,

$$S[\hat{\phi}, \phi] = -\sum_i \phi_i(t_f) + \int_0^{t_f} dt \sum_i (\hat{\phi}_i \partial_t \phi_i + H_i[\hat{\phi}, \phi]), \quad (13)$$

with Hamiltonian,

$$H_i = (1 - \hat{\phi}_i) e^{-\hat{\phi}_i \phi_i} \sum_{l=1}^{N-i} \prod_{j=1}^{l-1} J_{i,i+l}(l) \hat{\phi}_{i+l} \phi_{i+l} (1 - \phi_{i+j}) + \text{o.t.}, \quad (14)$$

where we summarized the hopping and left-nearest-neighbor interactions by o.t.

In order to evaluate the path integral, we define how the $\hat{\delta}$ operators in H act on the coherent-state basis by following the rules in Ref. [39],

$$\langle \phi | a_i^\dagger \hat{\delta}_{n_i,m_i} | \phi_i \rangle = \frac{1}{m_i!} \hat{\phi}_i (\hat{\phi}_i \phi_i)^{m_i} e^{-\phi_i \hat{\phi}_i},$$

$$\langle \phi | a_i \hat{\delta}_{n_i,m_i} | \phi \rangle = \frac{1}{(m_i - 1)!} \phi_i (\hat{\phi}_i \phi_i)^{m-1} e^{-\phi_i \hat{\phi}_i}$$

$$\langle \phi | \hat{\delta}_{n_i,m_i} | \phi \rangle = \frac{1}{m_i!} (\hat{\phi}_i \phi_i)^{m_i} e^{-\phi_i \hat{\phi}_i}. \quad (15)$$

Many different approaches have been proposed to deal with the particle exclusion enforced by the $\hat{\delta}$ operator. Examples of this are fermionic field theories [40] or more recent approaches using negative rates [41]. Here we will use the hard-bosonic path-integral approach [39]. The benefit of using this formalism is that it gives a characteristic length scale, which distinguishes different spatial regimes of the correlation function and which will be important for its calculation.

A. Semiclassical limit of the field theory

In order to obtain the moments of $P(\boldsymbol{\sigma}, t)$, we now derive the semiclassical solution of the field theory. To this end, we will evaluate the path integral in Eq. (12) for fields that make the action S extremal. This limit will be shown to be valid if the average enzyme occupancy is small.

Solutions to this model with *local* interactions are known or can easily be obtained using the methods we describe below [35,36]. Here we study interactions that are motivated by the interplay between enzyme binding and geometric changes of the substrate. For example, enzyme binding could compact the substrate, such that sites far away on the lattice are in close proximity in real space. Such interactions are therefore long-ranged in nature and we consider a general class of nonlocal interaction kernels of the form $J_{i,i+l} = 1/l^\gamma$. We also made the implicit assumption that the substrate reaches a steady state on much faster time scales compared to the enzyme processes. This is indeed the case in relevant biological contexts. For example, on the length scale on which DNA loops are unimportant, the local equilibration of the chromatin occurs orders

of magnitude faster than the epigenetic modifications thereof are established or removed during cell state transitions [42].

The exponent γ describes how rapidly the interaction strength decays along the substrate. In the special case that the substrate is a polymer in equilibrium, the exponent γ can be related to the exponent ν describing the statistics of the end-to-end distance. In three spatial dimensions, this relation reads $\gamma = (3 + g)\nu$, where g is an exponent describing the two-point distribution function at close distances [43]. For example, for compact polymers, the exponent describing the distance between two internal points is $\nu = 1/2$ [44], giving a value of $\gamma = 3/2$. This forms a lower bound for the exponent γ in a compact equilibrium polymer. A polymer in an extended form would yield a value of $\gamma \approx 5$. Different values of γ can be obtained for nonequilibrium substrates. For example, for a compacted substrate that does not fluctuate and is space filling the total binding rate of enzymes would scale as $L^{2/3}$, where L is the size of the substrate. As the total binding rate is the integral over the interaction kernel the exponent γ in this case would be $\gamma = 1/3$.

In the first step, we rewrite the Hamiltonian, Eq. (14), in continuous space with coordinate s. On introducing a spatial discretization $\sum_i \Delta s \to \int ds$, where Δs is the lattice spacing and s a continuous coordinate, the Hamiltonian in the action, Eq. (14) becomes

$$
\begin{aligned}
H[\hat{\phi}, \phi] = {} & J(1 - \hat{\phi}(s)) e^{-\phi \hat{\phi}} \\
& \cdot \left[\int_0^{N-s} dy \frac{\hat{\phi}(s+y)\phi(s+y)}{y^\gamma} e^{-\int_{z=0}^y dz \hat{\phi}(s+z)\phi(s+z)} \right. \\
& \left. + \int_0^s dy \frac{\hat{\phi}(s-y)\phi(s-y)}{y^\gamma} e^{-\int_{z=0}^y dz \hat{\phi}(s-z)\phi(s-z)} \right].
\end{aligned}
\quad (16)
$$

Here we choose the binding rates J_{ij} to be equal throughout the lattice, i.e., we do not consider disorder. As the integrals in Eq. (16), diverge for $\gamma \geqslant 1$, we henceforth require that $\gamma < 1$.

Expanding Eq. (16) to first order in the exponentials, to the second order in the terms $\hat{\phi}(s \pm y)\phi(s \pm y)/y^\gamma$ and extending the upper limit of integration to infinity the terms containing the integrals simplify to

$$\left[2(\hat{\phi}\phi)^\gamma + (\phi\hat{\phi})^{\gamma-3}(2 - 3\gamma + \gamma^2) \frac{\partial^2(\phi\hat{\phi})}{\partial s^2} \right]. \quad (17)$$

We now perform a semiclassical approximation of the generating functional by employing a saddle-point bifurcation of the path integral. To this end, we minimize the action, $\delta S/\delta \hat{\phi}(s)|_{\hat{\phi}(s)=1} = 0$, while setting $\hat{\phi}(s) = 1$ to ensure probability conservation (cf. Ref. [36]). With this, we obtain a partial differential equation describing the time evolution of the enzyme-binding profile along the substrate, $\phi(s)$, which for small values of $\phi(s)$ is

$$\frac{\partial \phi_0(s)}{\partial \tilde{t}} = e^{-\phi_0(s)} \{ \phi_0(s)^\gamma + [\mu \phi_0(s)^{\gamma-3} + \epsilon] \partial_s^2 \phi_0(s) \}. \quad (18)$$

Here we rescaled time according to $\tilde{t} = t 2J\Gamma(1 - \gamma)$ and defined $\mu = (2 - 3\gamma + \gamma^2)/2 > 0$, and indicated the mean-field approximation as ϕ_0. We reuse the symbol ϵ for the diffusion constant. The factor $e^{-\phi_0(s)}$ is a direct consequence of the
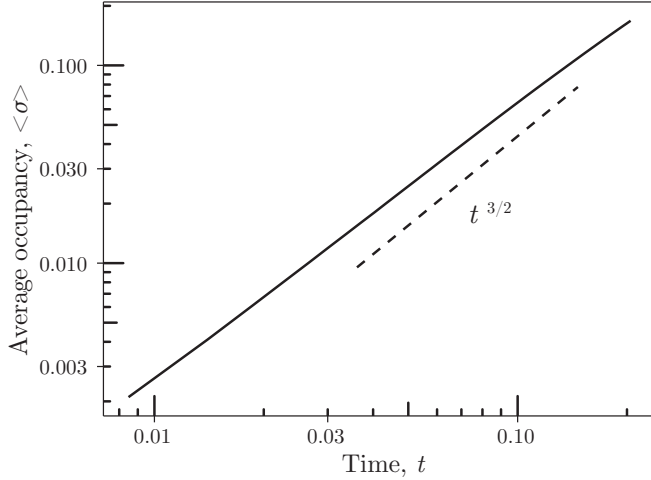
FIG. 2. Time evolution of the average enzyme occupancy obtained from stochastic simulations of the master equation (1) for $\gamma = 1/3$ and 10^7 lattice sites (solid line). The simulation was initialized with For early times, the theory predicts an increase following a power law with an exponent of 3/2 which is indicated by the dashed line.

site restriction, which intuitively has the role of preventing unbounded growth.

In the hard-boson path-integral representation, Eq. (16), the term $\exp[-\int_{z=0}^{y} dz \hat{\phi}(s+z)\phi(s+z)]$ in the Hamiltonian is approximated by an exponential of the space-averaged fields, $\exp[-y\langle\hat{\phi}(s)\phi(s)\rangle]$ if the fields are slowly varying. This defines an effective exponential cutoff of the interactions at a characteristic length $1/y^\gamma$. Because contributions from sites separated by a long distance are effectively suppressed, this justifies the expansion of the limit in Eq. (16) to ∞.

The first spatially homogeneous moment, $\phi_0(t)$, i.e., the average number of bound enzymes, $\langle\sigma\rangle$, is the solution of Eq. (18) when neglecting diffusion. We consider initial conditions that correspond to an almost empty substrate. Such initial conditions are relevant in the context of cell-state transitions. Examples include the *de novo* methylation of the DNA during early embryonic development or its erasure in erythropoiesis. With these initial conditions, the term $e^{-\phi}\phi^\gamma$ on the right-hand side of Eq. (18) is to first order well approximated by ϕ^γ. Therefore, at short times, the first moment follows a power law,

$$\langle\sigma\rangle \sim t^{\frac{1}{1-\gamma}}. \tag{19}$$

This is the first result of this manuscript. In Fig. 2 we compare the analytical solution to stochastic simulations using Gillespie's algorithm [45]. See Appendix B for details of the numerical implementation.

At large times, site exclusion becomes dominant and the solution approaches a steady-state solution, ϕ^*, logarithmically. The steady-state concentration of bound enzymes is determined by a balance between binding and unbinding events and it is given by

$$\phi^* = (1-\gamma)W\left(\frac{\bar{u}^{\frac{1}{\gamma-1}}}{1-\gamma}\right), \tag{20}$$

where W is the Lambert W function and $\bar{u} = u/[2J\Gamma(1-\gamma)]$ is the relative strength of unbinding and interactions. Therefore, if the coupling, J, is much larger than u, then the steady-state concentration of bound enzymes decreases with $\bar{u}^{-1/(1-\gamma)}$. In the limit that interactions are much weaker compared to degradation the steady-state concentration increases logarithmically, $\phi^* \sim \ln[\bar{u}^{-1/(1-\gamma)}]$.

Taken together, starting from an almost empty substrate, the average number of occupied binding sites increases following a power law up to a point where higher-order interactions due to site exclusion become dominant. As an example, for enzymes binding to a fully compacted, space-filling polymer, γ takes a value of 1/3 such that the number of bound sites increases with an exponent of 3/2.

As a remark, at the level of a mean-field description, we can map the enzyme-substrate model to a Smoluchowski equation [46] describing the size of domains where all sites are bound. In this view, a binding event between two already occupied sites is equivalent to a fragmentation event splitting the domain into two smaller intervals. Restricting our attention to the first moment, we can rewrite our model in the mean-field limit as a fragmentation equation,

$$\frac{\partial c(x)}{\partial t} = \int_0^\infty dy\, J(x, y-x)c(y) - c(x)\int_0^x dy\, J(y, x-y), \tag{21}$$

where $c(x, t)$ is the number of domains of size x at time t and we omitted the time-dependency for a shorter notation. For the chosen kernel, $J(x, y) = 1/x^\gamma + 1/y^\gamma$, and after defining the moments as $M_\alpha = \int dx\, c(x)x^\alpha$, we obtain $M_{\alpha+\gamma+1} \sim t^{-(\alpha+\gamma)/(\gamma+1)}$. The average occupancy, which is the zeroth moment, scales as $\langle\sigma\rangle \sim t^{1/(\gamma-1)}$. This equation gives the same time evolution of the number of enzymes bound to the substrate as the path-integral methods.

B. Correlation functions

To compute correlation functions and scaling exponents we need to take the derivative of the generating function (12). However, such an approach is not feasible for three reasons.

The first reason is that we would need to expand the action and this attempt fails due to the presence of a mass term in the field theory. Therefore, the field theory is not scale-invariant. In order to overcome this problem, we could try to do a change of variables in the action Eq. (16), and make a Hopf-Cole transformation around a dynamical mean field solution, such that in that reference frame the theory is massless. Even though the theory will be renormalizable, the exponent we get from such a calculation does not agree with the result of numerical simulations. The second reason why such an approach fails is that we would need to consider perturbations of any order in the field theory and a one-loop calculation would not be sufficient [47]. The third and main reason for the failure of this approach is that, after expanding around a base state, integrals of the form in Eq. (16) cannot be approximated without losing the length scale, $1/\langle\phi\rangle$, associated with the effective cutoff of the interactions.

The key insight to calculate the correlation function is that Eq. (16) gives rise to two spatial regimes: At short distances, interactions are long-ranged following a power law decay with

exponent $1/\gamma$ while for distances much larger than $1/\langle\phi\rangle$ interactions are effectively screened. In the following, we will therefore derive the correlation function separately for these two regimes using renormalization group methods and perturbation theory. We will then confirm these results with numerical simulations.

1. Short-distance regime

To describe the short-distance behavior of correlation functions, we start from the action, Eq. (16), and, after taking the semiclassical approximation, we expand it to first order in the fields and their derivatives,

$$\partial_t \phi(s,t) = \int_0^s dy\, \phi(y)|s-y|^{-\gamma} e^{-\int_{z=0}^{s-y} dz\, \phi(z)}$$
$$+ \int_0^s dy\, \partial_y \phi(y)|s-y|^{1-\gamma} e^{-\int_{z=0}^{s-y} dz\, \phi(z)}, \quad (22)$$

where s is again a continuous coordinate giving the position on the substrate. Here, for notation clarity, we omitted the noise terms, hopping terms, and integrals of the same form describing interactions with the right nearest bound site but we will consider them at the end of the derivation.

The interaction kernel Eq. (16) has the form $|s-y|^{-\gamma} e^{-\int_{z=0}^{s-y} dz\, \phi(z)}$, with $\gamma < 1$. By considering a perturbation $h(s,t)$ around the mean-field solution, $\phi_0(t)$, i.e., $\phi(s,t) = \phi_0(t) + h(s,t)$, Eq. (22) can be expressed to first order as

$$\partial_t \phi_0 + \partial_t h = e^{-\phi_0} \int_0^s dy\, \phi_0 |s-y|^{-\gamma} \left[1 - \int_0^{s-y} dz\, h(z) \right]$$
$$+ e^{-\phi_0} \int_0^s dy\, h(y)|s-y|^{-\gamma} \left[1 - \int_0^{s-y} dz\, h(z) \right]$$
$$+ \text{h.o.t.} \quad (23)$$

The first two terms of the integral on the right-hand side cancel with the first one on the left-hand side, which follows from the dynamical mean field solution, Eq. (18). Making a change of variables, $w = z + y$, we then obtain

$$\partial_t h = e^{-\phi_0} \int_0^s dy\, h(y)|s-y|^{-\gamma}$$
$$- e^{-\phi_0} \int_0^s dy \int_y^s dw\, h(y)|s-y|^{-\gamma} h(w-y) + \xi(s,t). \quad (24)$$

The second term on the right-hand side of Eq. (24) is the convolution of a fractional integral of a function and the function itself.

The noise term, $\xi(s,t)$, is Gaussian white noise. Its correlations can be derived from the field theory, Eq. (16), by identifying terms that are proportional to $\hat\phi^2$. In the expansion of the action, these terms comprise both nonconservative noise, which means that they are proportional to $\hat\phi^2$, and conservative noise, which means that they are proportional to $\hat\phi^2 \partial_s^2 \phi$. The perturbation $h(s,t)$ thus has both conservative and nonconservative components, such that we make the

following ansatz for the noise correlations:

$$\langle \xi(s,t)\xi(s',t') \rangle = \delta(t-t')(2\Gamma_{NC} - 2\Gamma_C \partial_s^2)\delta(s-s'). \quad (25)$$

Γ_C and Γ_{NC} are the noise strengths for conservative and nonconservative noise, respectively, which are functions of J only. We omit their dependency on the model parameters as this dependence does not influence the exponents of correlation functions.

Taken together, as the fractional integral scales in Fourier space as $q^{\gamma-1}$, a spatio-temporal perturbation in Fourier space follows a nonlinear Langevin equation of the form

$$\partial_t h(q,t) = (e^{-\phi_0(t)} q^{\gamma-1} - q^2)h(q,t)$$
$$- q^{\gamma-1} e^{-\phi_0(t)} h(q,t)^2 + \xi(q,t). \quad (26)$$

From the dynamical mean-field solution of the first moment, Eq. (18), we obtain, up to a prefactor, that $e^{-\phi_0} = e^{[-t^{1/(1-\gamma)}]}$. In the frequency domain, we hence obtain at small times, $t \to 0$ or $\omega \to \infty$, that

$$G_0^{-1} h(q,\omega) = -q^{\gamma-1} h(q,\omega)^2 + \xi(q,\omega), \quad (27)$$

where we have defined the inverse bare propagator as $G_0^{-1} = i\omega + q^2 - q^{\gamma-1}$. From the above equation, the bare correlations of h are then

$$C_0 = (2\Gamma_{NC} + 2\Gamma_C q^2)|G_0|^2. \quad (28)$$

Equation (27) is of second order and so admits an exact solution from which we calculate the two-point correlation function, $\langle h(q,\omega)h(q',\omega') \rangle$, where the average $\langle \ldots \rangle$ is performed over the noise.

In the short-distance regime, $q \to \infty$, we keep only leading-order terms in q. The leading order is given by the conservative noise, which scales as q^2 while nonconservative noise, which scales as q^0, becomes negligible. Performing the inverse Fourier transform we find that correlation functions asymptotically approach a power law,

$$\langle h(s,t)h(s',t) \rangle = \frac{\cos(\pi\gamma)(|s-s'|^2 \Gamma_C + \Gamma_{NC}\gamma(1+\gamma))}{\Gamma(\gamma)|s-s'|^{2+\gamma}}. \quad (29)$$

We therefore obtain for the scaling of the correlation function that

$$\langle h(s,t)h(s',t) \rangle \sim |s-s'|^{-\gamma}. \quad (30)$$

This result is intuitive as the spatial correlations are proportional to the exponent of the scale-free kernel J. This derivation is valid for low values of the average occupancy ϕ_0. We expect that for larger values of ϕ_0 higher-order corrections become relevant.

2. Long-distance regime

From the bare propagator and correlator in Eq. (28) we notice that, at large distances, second-order spatial derivatives dominate correlations, and due to nonconservative noise we expect correlation functions to be described by different exponents compared to the short-distance regime, where conservative noise was the leading contribution in the scaling, Eq. (29). The mean-field exponents can be estimated by dimensional analysis [36], where we compute the scaling of the

parameters in the action to make it dimensionless. Following these arguments, we find from Eq. (16) that the correlation function decays following a power law with exponent 2χ. According to this analysis, the value of the critical exponent χ in the long-distance regime should be $\chi = (-1 - d + \gamma)/3$, where d is the spatial dimension of the substrate. This follows from considering higher-order nonlinearities and it is the correct exponent for the long tail of the correlation function. In the following, we will rigorously derive the results of this scaling argument using dynamical renormalization group methods.

We begin with Eq. (22). After linearization it becomes

$$\partial_t h(s) = \partial_s^2 h(s) + \int_0^s dy\, h(y)|s-y|^{-\gamma}$$
$$- \int_0^s dy\, h(y)|s-y|^{1-\gamma}\left[h(s) - (s-y)\frac{1}{2}\partial_s h(s)\right]$$
$$+ \xi(s,t), \tag{31}$$

where we used that $\int_a^b ds\, f(s) \approx (b-a)(f(a) + f(b))/2$. Before proceeding with a renormalization procedure, we note that the nonlinearities of order h^2 in Eq. (31) can be relevant in this regime.

Because we approximated to linear order when obtaining Eq. (31) we must keep all the other quadratic terms in the field theory, Eq. (16). There is only one quadratic term which is,

$$(\hat{\phi} - 1)\phi\hat{\phi}\int_0^s dy\, \frac{\hat{\phi}(s-y)\phi(s-y)}{y^\gamma}e^{-\int_0^y dz\hat{\phi}(s-z)\phi(s-z)}. \tag{32}$$

However, after functional minimization of the action it cancels out with the term involving interactions with the right nearest neighbor. This is not surprising, because the model does not allow for field theories involving terms that break the space-reversal symmetry $s \to -s$. Taken together, by repeating the same calculations as before and including the additional term in Eq. (32) we obtain

$$\partial_t h(s) = \partial_s^2 h(s) + \int_0^s dy\, h(y)|s-y|^{-\gamma} \tag{33}$$
$$+ \frac{1}{2}\int_0^s dy\, h(y)|s-y|^{2-\gamma}\partial_s h(s) + \xi(s,t). \tag{34}$$

Considering both right and left nearest-neighbor interactions, the advective terms cancel out, again by the necessity to obey left-right symmetry. We then include the next highest-order term,

$$\partial_t h(s) = \partial_s^2 h(s) + \int_0^x dy\, h(y)|s-y|^{-\gamma}$$
$$+ \frac{1}{2}\partial_s^2 h(s)\int_0^s dy\, h(y)|s-y|^{2-\gamma} + \xi(s). \tag{35}$$

The following results apply to multidimensional systems. We therefore now generalize to any spatial dimension d by writing spatial coordinates in vector form, $\boldsymbol{s}$. In Fourier space,
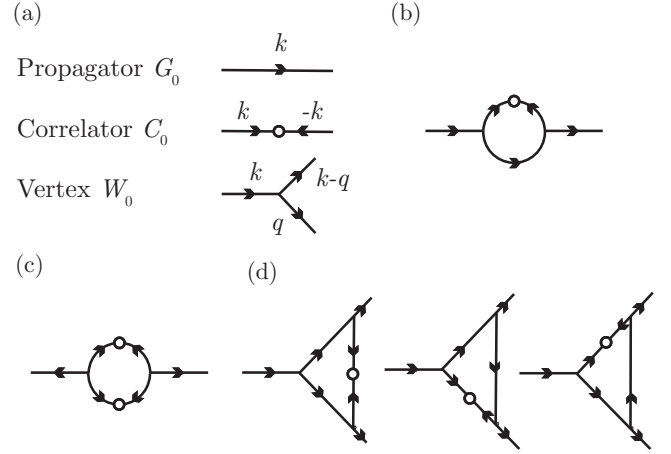

FIG. 3. (a) Overview of diagrammatical elements and diagrams contributing to the renormalization of the (b) propagator, (c) correlator, and (d) vertex functions. Every intersection corresponds to an integration over the wave vectors.

Eq. (35) can then be written in compact form,

$$G_0(\boldsymbol{q})^{-1}h(\boldsymbol{q},\omega) = -\mu\int_{\boldsymbol{k}} W(\boldsymbol{q},\boldsymbol{k})h(\boldsymbol{q},\omega)h(\boldsymbol{k}-\boldsymbol{q},\omega)$$
$$+ \xi(\boldsymbol{q},\omega), \tag{36}$$

where $h(\boldsymbol{q},t)$ is the Fourier transform of $h(\boldsymbol{s},t)$ and $\mu = (2 - 3\gamma + \gamma^2)/2$,

$$h(\boldsymbol{q},\omega) = \int ds \int dt\, h(\boldsymbol{s},t)e^{i\boldsymbol{q}\boldsymbol{s}}e^{i\omega t}. \tag{37}$$

We also defined the free propagator,

$$G_0^{-1} = i\omega + D\boldsymbol{q}^2 + J|\boldsymbol{q}|^{-\gamma}, \tag{38}$$

in which we reintroduced the dimensional parameters from the adimensional Eq. (36) in order to study their flow under renormalization. Finally, we defined the vertex, which accounts for the nonlinear terms, as

$$W(\boldsymbol{q},\boldsymbol{k}) = \frac{1}{2}\left[\frac{\boldsymbol{q}(\boldsymbol{k}-\boldsymbol{q})}{|\boldsymbol{k}-\boldsymbol{q}|^{3-\gamma}} + \frac{(\boldsymbol{k}-\boldsymbol{q})\boldsymbol{q}}{|\boldsymbol{q}|^{3-\gamma}}\right]. \tag{39}$$

In the hydrodynamic limit, $|\boldsymbol{k}| \to 0$ and $|\boldsymbol{q}| \to 0$, the vertex scales linearly with $|\boldsymbol{k}|$ and $|\boldsymbol{q}|$, which implies nonrenormalization of the vertex function.

The rescaling step of the renormalization group procedure then gives a rescaling of the form

$$\partial_l \epsilon = [z - 2 + A_D]\epsilon,$$
$$\partial_l \mu = [z + \chi - 2 + (3 - \gamma)]\mu,$$
$$\partial_l \Gamma_C = [z - 2\chi - d - 2 + A_{\Gamma_C}]\Gamma_C,$$
$$\partial_l \Gamma_{NC} = [z - 2\chi - d + A_{\Gamma_{NC}}]\Gamma_{NC}. \tag{40}$$

$A_{\Gamma_{NC}}$ and A_{Γ_C} depend on all of the parameters and need to be evaluated perturbatively by calculating the diagrams in Fig. 3.

Following standard calculations for the integrals represented by the diagrams in Fig. 3 [28], we recover the

renormalization-group flow for the parameters,

$$\partial_l \ln(\epsilon) = z - 2 - \frac{K_d \mu^2}{d\epsilon^3}[(d-2)\Gamma_{NC} + (d-3)\Gamma_C],$$

$$\partial_l \ln(\mu) = z + \chi - 2 + (3 - \gamma),$$

$$\partial_l \ln(\Gamma_C) = z - 2\chi - d - 2$$
$$- \frac{K_d \nu^2(1+d)(\Gamma_{NC} + \Gamma_C)^2}{2d\sigma_0^3 \Gamma_C},$$

$$\partial_l \ln(\Gamma_{NC}) = z - 2\chi - d, \tag{41}$$

where $K_d = S_d/(2\pi)^d$ and S_d is the surface area of a d-dimensional sphere.

The Galilean invariance of Eq. (36) leads to the nonrenormalization of the nonconserved noise and the couplings μ. This is similar to the renormalization of the KPZ-equation. As a result, we get the exact exponent identities $\chi = (-1 - d + \gamma)/3$ and $z = (-2 + d + 2\gamma)/3$. The dynamical exponent z governs the scaling of the average width, $w(t, L)$, of the field $h(s, t)$, $w(t, L) \sim L^{2\chi} f(t/L^z)$, where L is the system size. In $d = 1$, two-point spatial correlations functions then decay with an exponent $2(\gamma - 2)/3$ in the long-distance regime.

Taken together, we find that the correlation function along one-dimensional substrates decays in two algebraic regimes [Fig. 4(a)],

$$\langle h(s)h(s') \rangle = \begin{cases} |s - s'|^{-\gamma}, & \text{for } |s - s| \ll 1/\langle\sigma\rangle, \\ |s - s'|^{-\frac{2}{3}(2-\gamma)}, & \text{for } |s - s| \gg 1/\langle\sigma\rangle. \end{cases} \tag{42}$$

The crossover between these regimes stems from an effective exponential cutoff of the long-range interactions. The position of the crossover scales with the only length scale in the system, the typical distance between neighboring occupied sites, $1/\langle\sigma\rangle$, and, intuitively, separates a regime dominated by long-range interactions and a regime characterized by passive, conservative fluctuations.

Figure 4(b) shows the connected-correlation function, obtained from numerical simulation of Eq. (1) for the special case that $\gamma = 1/3$. To separately emphasize the short-distance and the long-distance regime we computed correlations at two levels of the average substrate occupancy. While we cannot confidently estimate the numerical exponent from the short-distance regime, the simulation data confirm the existence of a crossover and the exponent of $-10/9$ in the long-distance regime.

IV. DISCUSSION

In summary, we studied a stochastic enzyme-substrate model where binding events are correlated via long-range interactions. Such interactions mimic the effect of conformational changes in the substrate, where positions far apart along the substrate might be close in physical space. We employed a coherent-state path-integral representation of the master equation and renormalization-group theory to calculate the exponents describing the time evolution of the average occupancy and the correlation function.

We here studied the case, where long-range interactions are restricted to a finite distance. This is motivated both
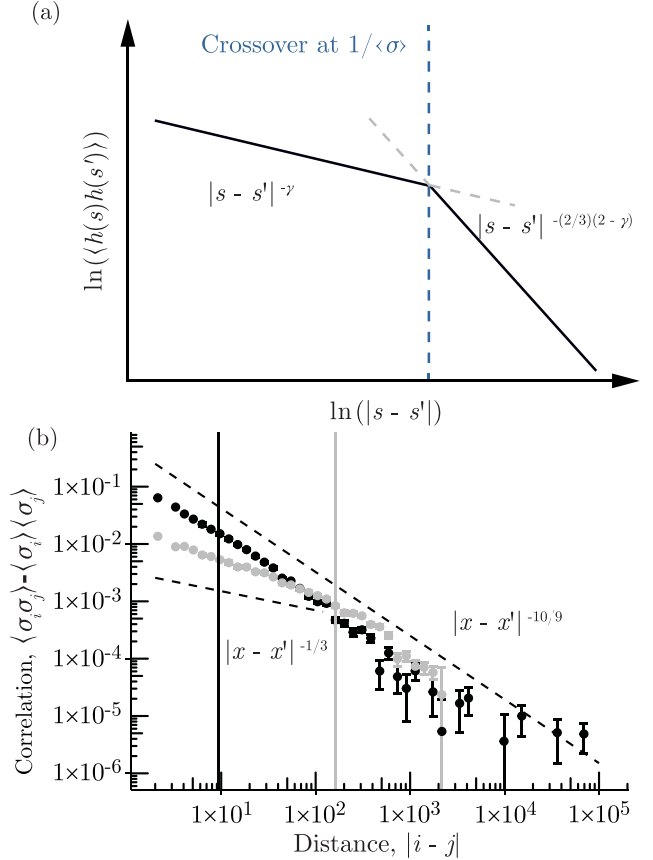

FIG. 4. (a) The two-point correlation function decays in two spatial regimes with exponents given by Eq. (42). The position of the crossover between both regimes increases with the typical length scale associated with the enzyme density, which scales as $1/\langle\sigma\rangle$. (b) Numerical simulation of the spatial correlation functions $\langle\sigma_i\sigma_j\rangle - \langle\sigma_i\rangle\langle\sigma_j\rangle$ for $\gamma = 1/3$ from stochastic simulations using Gillespie's algorithm with 10^7 lattice sites. We calculated the correlation function in two stages of the simulation: for an average occupancy probability of 0.006 (gray, emphasizing the short-distance regime) and an average occupancy of 0.108 (black, emphasizing the long-distance regime). The vertical lines indicate the corresponding crossover positions. Dashed lines indicate the predicted exponents in both regimes. We binned the data logarithmically and error bars indicate mean $\pm$ standard error. Note that the exponents for the fields $h(s)$, $\phi(s)$, and the lattice variable σ are identical.

from physical and biological arguments. An alternative model, where interactions are entirely unrestricted in range, is mathematically less challenging than the model analyzed here. In models with unrestricted long-range interactions, the theory is ill defined in the thermodynamic limit for exponents $\gamma < 1$ because the binding rate does not converge. For $\gamma < 3/2$ mean-field theory is correct and for unrestricted long-range interactions, we expect the first moment to increase exponentially and the correlation function to decay with a power law in a single spatial regime. For $\gamma > 3$ a model with local interactions aptly describes the dynamics [48].

Novel technologies in super-resolution microscopy can quantify the location of individual enzymes bound to membranes or the DNA [14]. Such technologies allow for the quantification of spatial correlation functions of bound

enzymes. Our work allows associating the spatio-temporal statistics of bound enzymes to the enzyme-substrate kinetics and spatial conformation of the substrate. Measuring the moments along the substrate in an experiment would therefore allow drawing conclusions about the underlying biochemical processes.

APPENDIX A: PATH INTEGRAL FORMULATION OF THE MASTER EQUATION

To construct the field theory we first note that we can formally write a solution of the master equation as

$$|P(t)\rangle = e^{-Ht}|P(0)\rangle, \qquad (A1)$$

where $|P(0)\rangle$ is the initial state (i.e., the probability distribution of enzyme binding profiles at time $t = 0$). The exponential factor can be rewritten as

$$e^{-Ht} = (1 - \Delta t H)^{\frac{t}{\Delta t}} = (1 - \Delta t H) \cdot (1 - \Delta t H) \cdots. \qquad (A2)$$

By inserting the identity in the coherent state basis between every factor on the right-hand side of Eq. (A1), we find that the solution for any time t_1 can be written as

$$|P(t_1)\rangle = \int \prod \sigma_i d\phi_i(t_1 + \Delta t) d\hat{\phi}_i(t_1 + \Delta t) d\phi(t_1) d\hat{\phi}_i(t_1)$$

$$\cdot e^{-\hat{\phi}_i(t_1)\phi(t_1)} \cdot e^{-\hat{\phi}_i(t_1+\Delta t)\phi(t_1+\Delta t)_i} \cdot e^{\phi_i(t_1+\Delta t)a^\dagger}$$

$$\cdot |0\rangle\langle 0|e^{\hat{\phi}_i(t_1+\Delta t)a}(1 - \Delta t H)e^{\phi_i(t_1)a^\dagger}|0\rangle\langle 0|e^{\hat{\phi}_i(t_1)a}. \qquad (A3)$$

In this equation, we have to evaluate quantities in the coherent state basis between the bra and the ket,

$$\langle 0|e^{\hat{\phi}_i(t_1+\Delta t)a}(1 - \Delta t H)e^{\phi_i(t_1)a^\dagger}|0\rangle$$

$$= e^{\hat{\phi}_i(t_1+\Delta t)}e^{\phi_i(t_1)} - \Delta t \langle 0|e^{\hat{\phi}_i(t_1+\Delta t)a}(H)e^{\phi_i(t_1)a^\dagger}|0\rangle$$

$$\approx e^{\hat{\phi}_i(t_1+\Delta t)}e^{\phi_i(t_1)}e^{-\Delta t H(\hat{\phi}_i(t_1),\phi_i(t_1))}, \qquad (A4)$$

where $H(\hat{\phi}_i, \phi_i)$ is obtained by replacing all a_i with ϕ_i and $a_i^\dagger$ with $\hat{\phi}_i$, using the previously introduced decomposition and by taking into account the rules for exclusion processes, Eq. (15). Repeating this procedure $t/\Delta t$ times for each factor $(1 - \Delta t H)$ we end up with an integral, over a product of three terms P_2, P_3, P_4. The integral is

$$\int \prod \sigma_i d\hat{\phi}_i(t) d\phi_i(t) \dots d\hat{\phi}_i(\Delta t) d\phi_i(\Delta t) d\hat{\phi}_i(0) d\phi_i(0), \qquad (A5)$$

which can be rewritten compactly as a functional integral $\int \mathcal{D}[\phi]\mathcal{D}[\hat{\phi}]$. P_2 is composed of a product of terms that can be rewritten utilizing Riemann integration,

$$P_2 = \prod_{t_1=\Delta t}^{t} e^{\hat{\phi}(t_1+\Delta t)\phi(t_1) - \hat{\phi}(t_1)\phi(t_1)} \approx e^{-\int dt\, \partial_t \hat{\phi}\phi}. \qquad (A6)$$

Finally, there are further $t/\Delta t$ terms coming from the Hamiltonian evaluated at each time step,

$$P_3 = \prod_{t_1=\Delta t}^{t} e^{-\Delta t H(\hat{\phi}(t_1),\phi(t_1))} \approx e^{-\int dt H(\hat{\phi}(t),\phi(t))}. \qquad (A7)$$

The final factor, P_4, represents initial conditions and we refer to Ref. [35] for a discussion of this term. With this, any observable can then be expressed as a path integral of the form

$$A(\boldsymbol{\sigma}) = \int \mathcal{D}[\phi]\mathcal{D}[\hat{\phi}]A(\boldsymbol{\phi}, \hat{\boldsymbol{\phi}} = 1)e^{-S[\hat{\phi},\phi]}, \qquad (A8)$$

with

$$S[\hat{\phi}, \phi] = -\sum_i \phi_i(t_f) + \int_0^{t_f} dt \sum_i (\hat{\phi}_i(t)\partial_t \phi_i(t) + H_i[\hat{\phi}, \phi]), \qquad (A9)$$

where we have performed a partial integration in time and

$$H_i[\hat{\phi}, \phi] = (1 - \hat{\phi}_i)e^{-\hat{\phi}_i\phi_i}\left(\sum_{l=1}^{N-i}\prod_{j=1}^{l-1} J_{i,i+l}(l)\hat{\phi}_{i+l}\phi_{i+l} \right.$$

$$\left. \times (1 - \phi_{i+j}) + \text{o.t.} \right). \qquad (A10)$$

Defining the generating functional of correlations, $Z[\boldsymbol{h}, \phi, \hat{\phi}]$, as

$$Z[\boldsymbol{h}, \phi, \hat{\phi}] = \int \mathcal{D}[\boldsymbol{h}, \phi, \hat{\phi}]e^{-S[\phi,\hat{\phi}]+\iint dsdt[h\phi+\hat{h}\hat{\phi}]}, \qquad (A11)$$

expectation values of products of observables, such as correlation functions, can then be expressed as functional derivatives with respect to the auxiliary external field,

$$\langle \phi(s, t)\phi(y, t')\rangle = \frac{\delta^2}{\delta h(s, t)\delta h(y, t)}Z[\boldsymbol{h}, \phi, \hat{\phi}]|_{\boldsymbol{h}=0}. \qquad (A12)$$

APPENDIX B: STOCHASTIC SIMULATIONS

To test the validity of our analytical results we perform extensive stochastic simulations by integration of the master equation Eq. (1) using Gillespie's algorithm [45] with 10^7 lattice sites, a random initial distribution of enzymes with an occupancy fraction equal to 10^{-4}, and interaction strength $J = 1$. Unbinding and hopping rates are set to zero as they do not affect the critical dynamics and would lead to significantly slower simulations. This is because the number of lattice sites needs to be large enough to measure the exponents of the spatial correlations.

[1] B. Alberts, D. Bray, J. Lewis, M. Raff, K. Roberts, and J. Watson, *Molecular Biology of the Cell*, 4th ed. (Garland, New York, 2002).

[2] C. Salazar and T. Höfer, Multisite protein phosphorylation—From molecular mechanisms to kinetic models, FEBS J. **276**, 3177 (2009).

[3] F. Reiter, S. Wienerroither, and A. Stark, Combinatorial function of transcription factors and cofactors, Curr. Opin. Genet. Dev. **43**, 73 (2017).

[4] G. Vilkaitis, I. Suetake, S. Klimašauskas, and S. Tajima, Processive methylation of hemimethylated cpg sites by mouse dnmt1 dna methyltransferase, J. Biol. Chem. **280**, 64 (2005).

[5] D. E. J. Koshland, Correlation of structure and function in enzyme action, Science **142**, 1533 (1963).

[6] Y. Savir and T. Tlusty, Conformational proofreading: The impact of conformational changes on the specificity of molecular recognition, PLoS ONE **2**, e468 (2007).

[7] J. Dekker and T. Misteli, Long-range chromatin interactions, Cold Spring Harb. Perspect. Biol. **7**, a019356 (2015).

[8] C. P. Broedersz, X. Wang, Y. Meir, J. J. Loparo, D. Z. Rudner, and N. S. Wingreen, Condensation and localization of the partitioning protein parb on the bacterial chromosome, Proc. Natl. Acad. Sci. USA **111**, 8809 (2014).

[9] G. David, J.-C. Walter, C. P. Broedersz, J. Dorignac, F. Geniet, A. Parmeggiani, N.-O. Walliser, and J. Palmeri, Phase separation of polymer-bound particles induced by loop-mediated one dimensional effective long-range interactions, Phys. Rev. Res. **2**, 033377 (2020).

[10] L. Connolley, L. Schnabel, M. Thanbichler, and S. M. Murray, Partition complex structure can arise from sliding and bridging of parb dimers, Nat. Commun. **14**, 4567 (2023).

[11] F. Olmeda, T. Lohoff, S. J. Clark, L. Benson, F. Krüger, W. Reik, and S. Rulands, Inference of emergent spatio-temporal processes from single-cellsequencing reveals feedback between de novo dna methylation and chromatin condensates, bioRxiv (2021).

[12] D. Michieletto, E. Orlandini, and D. Marenduzzo, Polymer model with epigenetic recoloring reveals a pathway for the de novo establishment and 3d organization of chromatin domains, Phys. Rev. X **6**, 041047 (2016).

[13] J. Schnitzbauer, M. T. Strauss, T. Schlichthaerle, F. Schueder, and R. Jungmann, Super-resolution microscopy with dna-paint, Nat. Protocols **12**, 1198 (2017).

[14] S. C. M. Reinhardt, L. A. Masullo, I. Baudrexel, P. R. Steen, R. Kowalewski, A. S. Eklund, S. Strauss, E. M. Unterauer, T. Schlichthaerle, M. T. Strauss, C. Klein, and R. Jungmann, Ångström-resolution fluorescence microscopy, Nature (London) **617**, 711 (2023).

[15] S. J. Clark, R. Argelaguet, C.-A. Kapourani, T. M. Stubbs, H. J. Lee, C. Alda-Catalinas, F. Krueger, G. Sanguinetti, G. Kelsey, J. C. Marioni, O. Stegle, and W. Reik, scNMT-seq enables joint profiling of chromatin accessibility DNA methylation and transcription in single cells, Nat. Commun. **9**, 781 (2018).

[16] C. Gawad, W. Koh, and S. R. Quake, Single-cell genome sequencing: Current state of the science, Nat. Rev. Genet. **17**, 175 (2016).

[17] I. Langmuir, The adsorption of gases on plane surfaces of glass, mica and pt, J. Am. Chem. Soc. **40**, 1361 (1918).

[18] C. W. Gardiner, *Handbook of Stochastic Methods for Physics, Chemistry and the Natural Sciences*, 3rd ed., Springer

[19] S. Reuveni, M. Urbakh, and J. Klafter, The role of substrate unbinding in michaelis-menten enzymatic reactions, Biophys. J. **106**, 677a (2014).

[20] M. J. Morelli, R. J. Allen, and P. R. t. Wolde, Effects of macromolecular crowding on genetic networks, Biophys. J. **101**, 2882 (2011).

[21] F. Jülicher and R. Bruinsma, Motion of rna polymerase along dna: A stochastic model, Biophys. J. **74**, 1169 (1998).

[22] G.-W. Li, O. G. Berg, and J. Elf, Effects of macromolecular crowding and dna looping on gene regulation kinetics, Nat. Phys. **5**, 294 (2009).

[23] M. Coppey, O. Bénichou, R. Voituriez, and M. Moreau, Kinetics of target site localization of a protein on DNA: A stochastic approach, Biophys. J. **87**, 1640 (2004).

[24] L. Mirny, M. Slutsky, Z. Wunderlich, A. Tafvizi, J. Leith, and A. Kosmrlj, How a protein searches for its site on DNA: The mechanism of facilitated diffusion, J. Phys. A: Math. Theor. **42**, 434013 (2009).

[25] A. Buchner, F. Tostevin, and U. Gerland, Clustering and optimal arrangement of enzymes in reaction-diffusion systems, Phys. Rev. Lett. **110**, 208104 (2013).

[26] A. Gupta, A. Milias-Argeitis, and M. Khammash, Dynamic disorder in simple enzymatic reactions induces stochastic amplification of substrate, J. R. Soc. Interface. **14**, 20170311 (2017).

[27] A. Altland and B. D. Simons, *Condensed Mmatter Field Theory* (Cambridge University Press, Cambridge, UK, 2010).

[28] J. Zinn-Justin, *Quantum Field Theory and Critical Phenomena*, 4th ed., International Series of Monographs on Physics (Clarendon Press, Oxford, 2002).

[29] F. Ginelli, H. Hinrichsen, R. Livi, D. Mukamel, and A. Politi, Directed percolation with long-range interactions: Modeling nonequilibrium wetting, Phys. Rev. E **71**, 026121 (2005).

[30] F. Ginelli, H. Hinrichsen, R. Livi, D. Mukamel, and A. Torcini, Contact processes with long range interactions, J. Stat. Mech. (2006) P08008.

[31] H. Hinrichsen, Non-equilibrium phase transitions with long-range interactions, J. Stat. Mech. (2007) P07006.

[32] F. Bouchet and J. Barré, Statistical mechanics of systems with long range interactions, in *Journal of Physics: Conference Series* (IOP, Philadelphia, PA, 2006), Vol. 31, p. 18.

[33] K. Sneppen and I. B. Dodd, Nucleosome dynamics and maintenance of epigenetic states of cpg islands, Phys. Rev. E **93**, 062417 (2016).

[34] M. A. Ricci, C. Manzo, M. F. García-Parajo, M. Lakadamyali, and M. P. Cosma, Chromatin fibers are formed by heterogeneous groups of nucleosomes in vivo, Cell **160**, 1145 (2015).

[35] J. Cardy, G. Falkovich, and K. Gawedzki, in *Non-equilibrium Statistical Mechanics and Turbulence*, edited by S. Nazarenko and O. V. Zaboronski, London Mathematical Society Lecture Note Series (Cambridge University Press, Cambridge, UK, 2008).

[36] U. C. Täuber, *Critical Dynamics: A Field Theory Approach to Equilibrium and Non-Equilibrium Scaling Behavior* (Cambridge University Press, Cambridge, UK, 2014).

[37] M. Doi, Second quantization representation for classical many-particle system, J. Phys. A: Math. Gen. **9**, 1465 (1976).

Series in Synergetics Vol. 13 (Springer-Verlag, Berlin, 2004), pp. xviii+415.

[38] L. Peliti, Path integral approach to birth-death processes on a lattice, J. Phys. **46**, 1469 (1985).

[39] F. van Wijland, Field theory for reaction-diffusion processes with hard-core particles, Phys. Rev. E **63**, 022101 (2001).

[40] V. Brunel, K. Oerding, and F. van Wijland, Fermionic field theory for directed percolation in (1+1)-dimensions, J. Phys. A: Math. Gen. **33**, 1085 (2000).

[41] S. Nekovar and G. Pruessner, A field-theoretic approach to the wiener sausage, J. Stat. Phys. **163**, 604 (2016).

[42] C. P. Johnstone, N. B. Wang, S. A. Sevier, and K. E. Galloway, Understanding and engineering chromatin as a dynamical system across length and timescales, Cell Syst. **11**, 424 (2020).

[43] S. Redner, Distribution functions in the interior of polymer chains, J. Phys. A: Math. Gen. **13**, 3525 (1980).

[44] R. Lua, A. L. Borovinskiy, and A. Y. Grosberg, Fractal and statistical properties of large compact polymers: A computational study, Polymer **45**, 717 (2004).

[45] D. T. Gillespie, A general method for numerically simulating the stochastic time evolution of coupled chemical reactions, J. Comput. Phys. **22**, 403 (1976).

[46] P. L. Krapivsky, S. Redner, and E. Ben-Naim, *A Kinetic View of Statistical Physics* (Cambridge University Press, Cambridge, UK, 2010).

[47] H.-K. Janssen, F. van Wijland, O. Deloubrière, and U. C. Täuber, Pair contact process with diffusion: Failure of master equation field theory, Phys. Rev. E **70**, 056114 (2004).

[48] C. Behan, L. Rastelli, S. Rychkov, and B. Zan, Long-range critical exponents near the short-range crossover, Phys. Rev. Lett. **118**, 241601 (2017).